https://doi.org/10.5194/egusphere-2025-324
Preprint. Discussion started: 17 February 2025

Interaction mechanism between the karst aquifer and stream under precipitation infiltration recharge

Fuyun Huang[1], Yuan Gao[1*], Xiaonong Hu[2], Xiaoguang Wang[3,4], Shengyan Pu[5]

1. School of Geology and Mining Engineering, Xinjiang University, Urumqi, Xinjiang 830046, China

2. School of Water Conservancy and Environment, University of Jinan, Jinan, Shandong 250022, China

3. State Key Laboratory of Oil and Gas Reservoir Geology and Exploitation, Chengdu University of Technology, Chengdu, Sichuan 610059, China

4. Tianfu Yongxing Laboratory, Chengdu, Sichuan 610059, China

5. State Key Laboratory of Geohazard Prevention and Geoenvironment Protection, Chengdu University of Technology, Chengdu, Sichuan 610059, China

*Correspondence to Yuan Gao (yuangao_xju@hotmail.com)

Abstract: The variation in seasonal precipitation intensity impacts the dynamic interaction between the karst aquifer and stream. However, the interaction mechanism between the karst aquifer and stream is currently still unclear, and characterizing the impact of dynamic saturation process of groundwater in karst media on the interaction process remains a challenge. To delve into the impacts of varying precipitation intensities, different water retention models, multi-stage conduit arrangements, and multiple precipitation events on the interaction process between the karst aquifer and stream, this study employs the multiphase Darcy-Brinkman-Stokes equation to analyze the interaction process between the karst aquifer and stream. Additionally, the Phase Indicator Function is used to capture the dynamic changes in saturation levels of various media, and the Brooks-Corey (BC) and van Genuchten-Mualem (VGM) equations are

https://doi.org/10.5194/egusphere-2025-324
Preprint. Discussion started: 17 February 2025

employed to characterize the soil-properties of porous media. The results show that as the intensity of precipitation increases, the interaction process between the karst aquifer and stream becomes more complex, involving the synergistic recharge of multi-media and dynamic interactions with the karst aquifer. Discharges in both upper (PM I) and lower (PM II) porous media rise with precipitation intensity, but PM II shows a more significant increase and earlier peak discharge. Secondly, during the middle to late stages of precipitation, the discharge predicted by the BC model exceeds that of the VGM model. The multi-stage conduit arrangement significantly affects stream and karst conduit hydrology during heavy precipitation but has less impact on other media. Finally, multiple precipitation events with different intensities could affect the ease of recharge from media in different strata of the karst aquifer. The Darcy-Brinkman-Stokes model can effectively simulate the interaction process between the karst aquifer and stream under the influence of precipitation. It can accurately depict the two-phase interactive flow between various media controlled by the dynamic saturation process, and reveal the dynamic interaction process between karst aquifers affected by the epikarst, sinkholes, and conduits under infiltration recharge and stream. Meanwhile, it can precisely explain the processes of infiltration, overflow, and recession.

Keywords: the karst aquifer and stream; precipitation recharge; two-phase flow; Darcy-Brinkman-Stokes equation; interaction mechanism

https://doi.org/10.5194/egusphere-2025-324
Preprint. Discussion started: 17 February 2025

1. Introduction

Karst aquifer is not only a repository of substantial freshwater resources (Li et al., 2017; Ford & Williams, 2007; Sivelle et al., 2021), but also provides drinking water for 10% to 25% of the global population (Longenecker et al., 2017; Goldscheider et al., 2020; Mahler et al., 2021). However, karst-developed areas feature intricate pore structures and fractures (Kuniansky, 2016), leading to pronounced heterogeneity and anisotropy in the movement and storage of water within them (Zhang et al., 2020). In particular, the complex coupled flow involving various flow paths such as karst conduits, sinkholes, and epikarst, along with porous media, further intensifies the nonlinear recharge and discharge processes and the formation of preferential flow paths in the karst aquifer. With seasonal variations in precipitation intensity, the heterogeneity of the groundwater flow field is further exacerbated, and water levels in the karst aquifer and stream fluctuate, leading to complex interactions between the aquifer and stream (Bonacci, 2015). Unveiling the interaction mechanism between the karst aquifer and stream under varying precipitation intensities is crucial for assessing the storage of water resources in karst regions (Gao et al., 2021; Guo and Jiang, 2020).

The interaction process between the karst aquifer and stream is significantly influenced by karst media. In epikarst where the soil layer is shallow and dissolution weathering is pronounced, most precipitation can directly recharge the karst aquifer (Lee and Krothe, 2001; OLello et al., 2018). Karst conduits and sinkholes are important media involved in karst hydrological cycle. As rapid discharge channels, the size,

https://doi.org/10.5194/egusphere-2025-324
Preprint. Discussion started: 17 February 2025

connectivity, and distribution of karst conduits have a significant impact on karst hydrological processes (Duran et al., 2020; Bittner et al., 2020). Surface water collected into sinkholes can directly recharge the karst aquifer (Bianchini et al., 2022), thereby regulating the water level of the aquifer and the discharge volume to the stream, which is influenced by precipitation intensity, size and distribution of sinkhole. The permeability of sinkholes and conduits typically exhibits multilevel characteristics and varies with scale (Halihan et al., 1999), meaning there are strata structures with different permeabilities, which complicates the flow of water within the karst aquifer and increases the catchment area. Therefore, the recharge items to the stream adjacent to the karst aquifer usually include direct precipitation recharge, lateral runoff from the epikarst, discharge from karst springs, and recharge through porous media base flow.

The interaction process between the karst aquifer and stream is also regulated by the dynamic saturation process within the aquifer. The degree of dynamic saturation in different media determines the path and velocity of water flow. Unsaturated aquifers gradually saturate the underlying aquifers under the influence of gravity, while saturated underlying aquifers can cause water to overflow (Worthington, 1991; Huang et al., 2024). In addition, the dynamic saturation processes within the karst aquifer are regulated by factors such as seasonal water level fluctuations, the infiltration and flow of groundwater, and the periodic filling and draining of karst conduits (Huang et al., 2024).

Numerical methods are commonly employed as effective means to accurately

https://doi.org/10.5194/egusphere-2025-324
Preprint. Discussion started: 17 February 2025

simulate karst groundwater movement and assess karst groundwater resources. Shoemaker et al. (2008) proposed a method that discretely embeds conduits, connected by nodes, into the porous media grid (MODFLOW-CFP). This method not only evaluates the water resources of the entire karst aquifer but also considers the geometric shape and distribution of karst conduits on the hydrological processes. Estimations of karst groundwater movement and storage worldwide rely on this method (Kavousi et al., 2020; Qiu et al., 2019; Gao et al., 2020, 2024). Although MODFLOW-CFP is relatively comprehensive for regional karst groundwater simulation studies, it is necessary to couple seepage (porous media) with free flow (conduits and stream) and to describe the dynamic saturation process of the karst aquifer. This can be achieved by using the Navier-Stokes (N-S) equations to couple free flow with seepage through additional source terms (Soulaine and Tchelepi, 2016 ;Carrillo et al., 2020). The Phase Indicator Function for two-phase flow, combined with the phase transition method, can effectively describe the variable saturation process within the karst aquifer (Huang et al., 2024; Zhai et al., 2024). The Darcy-Brinkman-Stokes equations have been utilized to couple seepage flow and free flow (Huang et al., 2024; Nillama et al., 2022; Carrillo et al., 2020). Lu et al. (2023) analyzed a model that integrates fast discharge channels in fractures and conduits with slow seepage in porous media . The results demonstrate that the Darcy-Brinkman-Stokes equations can effectively describe two-phase flow in karst aquifers, and Soulaine (2024) proposed that mixed-scale models based on the Darcy-Brinkman-Stokes equations have strong potential for simulating coupled

https://doi.org/10.5194/egusphere-2025-324
Preprint. Discussion started: 17 February 2025

processes in porous systems. The karst aquifer are typically accompanied by turbulent flow. Reimann et al. (2011) conducted thorough research on turbulent flow in the karst aquifer. To reflect the dissipation of turbulent processes throughout the system, the N-S and Darcy-Brinkman-Stokes equations can be studied using the Reynolds Averaged Network System (RANS) method, where the k-ε turbulence model effectively characterizes turbulent flows in porous media, as demonstrated by del Jesus et al. (2012). The RANS method has been progressively refined for evaluating turbulent flow in both free-flow regions and porous media (Huang et al., 2024; Zhai et al., 2024; Higuera et al., 2014).

Currently, the interaction mechanism between the karst aquifer and stream during precipitation infiltration remains unclear, particularly how varying saturation levels in different karst media affect this interaction. Additionally, existing numerical methods fall short in accurately depicting the combined recharge processes across these diverse media within the karst aquifer. To better understand the interaction mechanisms between the karst aquifer and stream during precipitation infiltration, this study employs the Darcy-Brinkman-Stokes equations to model the coupled processes of seepage in porous media and free flow in karst conduit and stream. The Brooks-Corey (BC) and van Genuchten-Mualem (VGM) models are used to characterize the unsaturated seepage in karst media. The Volume of Fluid (VOF) method is applied to monitor the dynamic changes in aquifer saturation. This research elucidates how saturation dynamics in different karst media impact the coordinated recharge among

https://doi.org/10.5194/egusphere-2025-324
Preprint. Discussion started: 17 February 2025

media during precipitation infiltration, and examines the evolving interaction between the karst aquifer and stream under such recharge conditions. Given the complexity of the interaction mechanism between the karst aquifer and stream, this study specifically investigates the impact of four factors on the interaction mechanism: (1) changes in precipitation intensity, (2) different water retention models, (3) multi-stage conduit arrangements, and (4) multiple precipitation events. This study elucidates the interaction mechanisms between the karst aquifer and the stream under variable precipitation intensity recharge with seasonal changes, offering a scientific basis for the precise assessment of karst groundwater movement and storage.

2. Materials and methods

The study examines the interaction between karst aquifer and stream, as well as groundwater flow through various karst media, involving the coupling of seepage and free flow processes. Therefore, the Darcy-Brinkman-Stokes equations are adopted as the governing equations to describe the groundwater flow between the karst aquifer and stream, as well as within the karst media. The VOF phase transition method is applied to depict the two-phase flow of water and air in the media, and different water retention models are employed to characterize the unsaturated flow process of karst groundwater.

2.1 Mathematical model for simulating interaction process

The Darcy-Brinkman-Stokes equations are utilized to couple seepage flow in porous media with free flow in conduit and stream (Carrillo et al., 2020; Huang et al., 2024; Soulaine, 2024; Lu et al., 2023). The two-phase flow is captured using a phase

https://doi.org/10.5194/egusphere-2025-324
Preprint. Discussion started: 17 February 2025

indicator function. Additionally, the k-ε turbulence model is employed to characterize the turbulent flow features in both porous media seepage within the aquifer and free flow in conduit and stream.

$$\nabla \cdot v_t = 0 \tag{1}$$

$$\frac{\partial \rho \alpha_l}{\partial t} + \nabla \cdot (\alpha_l v_t) + \nabla \cdot (\varphi \alpha_l \alpha_g v_{rt}) = 0 \tag{2}$$

$$\frac{1}{\varphi}\left((1+c)\frac{\partial \rho v_t}{\partial t} + \nabla \cdot \left(\frac{\rho}{\varphi} v_t v_t\right)\right) = -\nabla p^* + \rho g \cdot X + \nabla \cdot \left(\mu_{eff}(\nabla v_t + \nabla {v_t}^T)\right) - \mu_{eff} k^{-1} v_t + F_c. \tag{3}$$

where t denotes the calculation time $[s]$ and φ the porosity; $\alpha_l = \frac{V_l}{V_g+V_l}$ is the aqueous-phase saturation, $\alpha_g = \frac{V_g}{V_g+V_l}$ is the gas-phase saturation, and V_g and V_l are the gas-phase and the aqueous-phase volumes, respectively; v_t is the fluid flow rate $[m/s]$; v_{rt} is the relative velocity between groundwater and air $[m/s]$; μ_{eff} is the effective viscosity that It can be defined as μ_{eff}, μ is the viscosity $[\mathrm{m}^2/s]$, $\mu = \alpha_g \mu_g + \alpha_l \mu_l$, and μ_g and μ_l are the viscosity of the gas and liquid phases, respectively; v_{turb} is the turbulent kinetic viscosity; ρ represents the average density of groundwater and air ; p^* is pressure $[pa]$; g is the gravitational acceleration, 9.81 $[\mathrm{m}^2/s]$; k is the permeability $[m^2]$; and F_c is the surface tension.

The eddy viscosity is expressed as:

$$\mu_t = \rho C_\mu \frac{k^2}{\varepsilon} \tag{4}$$

where k represents the turbulent kinetic energy, ε is the dissipation rate of turbulent kinetic energy, and C_μ is a constant , equal to 0.09.

Phase Indicator Function can be expressed as:

https://doi.org/10.5194/egusphere-2025-324
Preprint. Discussion started: 17 February 2025

$$\alpha_l = \begin{cases} 1 & \text{water} \\ 0 < \alpha < 1 & \text{two-phase zone} \\ 0 & \text{air} \end{cases} \tag{5}$$

where α_l represents the saturation of groundwater. Relative permeability is key to describing the migration of groundwater and gas (Kuang and Jiao, 2011). In relative permeability model for two-phase flow, the effective saturation of the aqueous phase, $\alpha_{l,e}$, is given by:

$$\alpha_{l,e} = \frac{\alpha_l - \alpha_{l,r}}{1 - \alpha_{g,r} - \alpha_{l,r}} \tag{6}$$

where, $\alpha_{l,r}$ and $\alpha_{g,r}$ are the residual saturations of water and air, respectively. In the Brooks and Corey (BC) model, the expression for the relative permeability k_r is given by (Brooks and Corey et al., 1964):

$$k_{r,g} = \left(1 - \alpha_{l,e}\right)^{0.5}\left(1 - \alpha_{l,e}^{1/m}\right)^{2m} \tag{7}$$

$$k_{r,l} = \alpha_{l,e}^{0.5}\left(1 - \left(1 - \alpha_{l,e}^{1/m}\right)^{m}\right)^{2} \tag{8}$$

where, m is a dimensionless parameter that is determined based on the characteristics of the porous media within the karst aquifer. The expression for relative permeability in the van Genuchten–Mualem (VGM) model (Parker et al., 1987) is defined as follows:

$$k_{r,g} = \left(1 - \alpha_{l,e}\right)^{0.5}\left(1 - \alpha_{l,e}^{1/m}\right)^{2m} \tag{9}$$

$$k_{r,l} = \alpha_{l,e}^{0.5}\left(1 - \left(1 - \alpha_{l,e}^{1/m}\right)^{m}\right)^{2} \tag{10}$$

In the free and porous regions, the source term μk^{-1} in the Darcy-Brinkman-Stokes equation varies in form and can be expressed as (Soulaine, 2024; Huang et al., 2024):

$$\mu_{eff} k^{-1} = \rho \boldsymbol{v}_{turb} k^{-1} + \begin{cases} 0, & \text{free region} \\ k_0^{-1}\left(\dfrac{k_{r,l}}{\mu_l} + \dfrac{k_{r,g}}{\mu_g}\right)^{-1}, & \text{porous region} \end{cases} \tag{11}$$

https://doi.org/10.5194/egusphere-2025-324
Preprint. Discussion started: 17 February 2025

The permeability coefficient k_0, which is determined by the geometric structure of the porous medium, controls both free flow and seepage. When permeability is high, the governing equation (Equation 3) simplifies to the Navier-Stokes equation (Equation 12). Conversely, when permeability is low, the equation reduces to Darcy's law (Equation 13).

$$(1+c)\frac{\partial \rho v_t}{\partial t} + \nabla\cdot(\rho v_t v_t) = -\nabla p^* + \rho g\cdot X + \nabla\cdot\left(\mu_{eff}(\nabla v_t + \nabla {v_t}^T)\right) + F_c, \text{if } \varphi = 1. \tag{12}$$

$$0 = -\nabla p^* + \rho g\cdot X - \mu_{eff}k^{-1}v_t + F_c, \text{if } \varphi \in]0,1[. \tag{13}$$

Meanwhile, the surface tension F_c and density ρ in the free-flow and porous media regions are as follows (Huang et al., 2024):

$$F_c = \begin{cases} -\dfrac{\sigma}{\varphi}\nabla\cdot\left(\dfrac{\nabla\alpha_l}{|\nabla\alpha_l|}\right)\nabla\alpha_l, & \text{free region} \\ \left[k_0\dfrac{\left(\dfrac{k_{r,l}}{\mu_l}\alpha_g - \dfrac{k_{r,g}}{\mu_g}\alpha_l\right)}{\dfrac{k_{r,l}}{\mu_l}+\dfrac{k_{r,g}}{\mu_g}}\left(\dfrac{\partial p_c}{\partial\alpha_l}\right) - p_c\right]\nabla\alpha_l, & \text{porous region} \end{cases} \tag{14}$$

$$\rho = \begin{cases} \rho_l\alpha_l + \rho_g\alpha_g, & \text{free regions} \\ k_0\dfrac{\left(\rho_g\dfrac{k_{r,g}}{\mu_g} + \rho_l\dfrac{k_{r,l}}{\mu_l}\right)}{\dfrac{k_{r,l}}{\mu_l}+\dfrac{k_{r,g}}{\mu_g}}, & \text{porous regions} \end{cases} \tag{15}$$

where σ is the interfacial tension $[N/m]$, p_c is capillary pressure $[pa]$.

$$k_{r,g} = (1-\alpha_{l,e})^{0.5}\left(1-\alpha_{l,e}^{\frac{1}{m}}\right)^{2m} \tag{16}$$

Numerical modeling

2.2 Numerical modelling

https://doi.org/10.5194/egusphere-2025-324
Preprint. Discussion started: 17 February 2025

The numerical model is developed according to the conceptual model of the karst aquifer adjacent to a stream, as depicted in Fig. 1. The model incorporates the distinctive features of karst regions, including sinkholes, epikarst, and karst conduit (Fig. 1). The karst conduit is connected to the epikarst through a sinkhole. The outcrop of the karst spring is located at the end of the karst conduit, directly leading to the stream. In the karst aquifer, the saturation levels within the porous media are dynamically altered by precipitation, and the water levels in both the karst conduit and the stream experience substantial fluctuations. As a result, the interaction between the porous media and the stream displays a clear multi-scale characteristic. From a hydrological perspective of the watershed, the recharge and discharge processes of karst conduit are controlled by the saturation degree of the surrounding porous media and the water level within the conduit themselves. Based on spatial relationships, the area between the karst conduit and the epikarst is divided into Porous Medium I (PM I) above the conduit, Porous Medium II (PM II) on the sides, and Porous Medium III (PM III) directly below the conduit. During a single precipitation event, some of the rainfall directly replenishes the stream, while the remainder percolates down to recharge the karst aquifer. The infiltration recharge consists of two processes: (1) infiltration recharge to the epikarst, and (2) downward infiltration recharge to the aquifer through sinkhole and porous media. These two processes sequentially recharge the stream: groundwater discharges laterally through the epikarst to the stream; precipitation rapidly recharges the connected karst conduit through the sinkhole and recharges to the stream through

https://doi.org/10.5194/egusphere-2025-324
Preprint. Discussion started: 17 February 2025

the karst spring, while groundwater in the aquifer also discharges laterally to the stream. Compared to PM I, groundwater in the epikarst recharges the stream at a faster rate, causing the water level of stream to rise and subsequently recharging PM I and PM II. As the water level of stream gradually rises, the stream will recharge the karst aquifer. Due to the rapid flow velocity of the stream, the water level drops, allowing groundwater in the lower porous media to discharge back into the stream. This study constructs a numerical model based on the dynamic interaction process between the karst aquifer and stream, revealing the interaction mechanism between the karst aquifer and stream under the influence of precipitation intensity changes, different water retention models, multi-level permeability arrangements, and multiple precipitation events.

The upper boundary of the strata is a transient natural precipitation boundary condition. The boundary condition for precipitation infiltration recharge is adopted using the following equation (Huang et al., 2024):

$$I(t) = \frac{b}{\sqrt{2\pi\sigma^2}} \sum e^{-\frac{\left(\frac{t_i-\mu}{a}\right)^2}{2\sigma^2}} \quad (17)$$

where t_i represents the time of the ith precipitation event, and $I(t)$ represents the total precipitation at that moment. According to Chang et al. (2015), μ, σ^2 and a are set as constants (90, 1.5 and 20, respectively). During precipitation infiltration recharge, changes in precipitation intensity are adjusted via the dimensionless parameter b.

Some researchers have positioned the karst conduit at the bottom of the model grid (Kavousi et al., 2020; Li et al., 2023). This study employs a programming approach to

https://doi.org/10.5194/egusphere-2025-324
Preprint. Discussion started: 17 February 2025

dynamically generate the sinkhole and conduit grids, enabling the creation of conduit and sinkhole of varying diameters at any position within the model by adjusting parameters such as conduit radius and center coordinates. This enhances the adaptability and practicality of the model.

Figure 2 illustrates the discretization scheme adopted by this study, clearly showing the division and distribution of grids in each region. Based on the thickness of the epikarst layer and the position of the stream, except for the stream, sinkhole, epikarst, and karst conduit, and the remaining areas are divided into porous media regions, and the grids in the free-flow regions are further refined. Given that the flow in the conduit, sinkhole, and stream is free-flowing, fine grids are required to capture the microscopic changes in water levels and interfaces, so the grids in these regions are locally refined. In the porous media, groundwater flows in a seepage manner, with its velocity decreasing with the increase in distance from the discharge end, forming a funnel-shaped pressure drop flow characteristic. Thus, a grid spacing approach with gradual increments in the porous media regions is employed. The edge grids are designed to be twice as long as those near the conduit. This method ensures precise simulation of flow near the discharge end while significantly reducing computational resource usage in distant areas. Given the dissolution effects near the sinkholes and epikarst, the permeability of the porous media in the karst aquifer decreases from the interior to the exterior, and it is assigned in a graded manner. The values of the model parameters are listed in Table 1.

https://doi.org/10.5194/egusphere-2025-324
Preprint. Discussion started: 17 February 2025

3. Results

3.1 Interaction process between the karst aquifer and stream under precipitation infiltration recharge

The changes in hydrological process curves, water level fluctuations, and their differences during the interaction between karst media and stream under different precipitation intensities are shown in Fig. 3. In the early stage of precipitation, the flow in the stream primarily originates from direct precipitation recharge and lateral groundwater recharge from epikarst (Fig. 3(a)). As the water level in the stream gradually rises, the flow not only continues downstream but also begins to recharge the karst aquifer, particularly the PM II. The peak recharge to PM II coincides with the peaks of epikarst recharge to the stream (Epikarst in Fig. 3) and direct precipitation recharge (P-River in Fig. 3). Therefore, the interaction process between the karst aquifer and stream during the early precipitation stage is significantly influenced by lateral groundwater discharge from the epikarst and the direct precipitation recharge. As groundwater recharge from epikarst to the stream declines (Fig. 3 (a)), groundwater moves downward through the epikarst to PM I, and begins to gradually recharge the stream. Due to the low permeability of the epikarst, lateral discharge from PM I to the stream will be delayed. During this process, the discharge volume of PM I exhibits two distinct peaks. The first peak is due to the recharge of groundwater from the epikarst, while the second peak is caused by the gradual saturation of PM II and the karst conduit, with a proportion of groundwater overflowing from PM I and discharging laterally to

https://doi.org/10.5194/egusphere-2025-324
Preprint. Discussion started: 17 February 2025

the stream. After the end of precipitation recharge, the hydrological process curve of PM I rapidly declined, and the discharge volume of the karst conduit, PM III and PM II gradually increase, causing the water level in the stream to rise (Fig. 3 (d)). When the water level in the stream gradually exceeds that of PM I, the stream begins to gradually recharge PM I. The karst conduit, PM II and PM III continue to discharge to the stream during this stage due to higher internal water pressure, forming a local hydrological cycle with the upper layer. In the late stage of precipitation, the hydrological process of the stream primarily shows a gradual decline in baseflow.

As depicted in Figs. 3b and 3c, the recharge and discharge dynamics between the karst aquifer and stream across different media shift notably with escalating precipitation intensity. The recharge volumes from the stream to PM I and PM II both decrease. The reduction in the recharge to PM II from the stream is primarily due to the acceleration of groundwater movement downward as precipitation intensity increases, causing groundwater to move more rapidly to the bottom of the karst aquifer, thereby recharging PM II. Consequently, part of pore space that should have been recharged by the stream is instead recharged from PM I downward. The decrease in the recharge to PM I can be attributed to its high internal saturation level and the rise in water level. On the other hand, the water level in the stream does not significantly exceed that of the upper aquifer, making it difficult for the stream to effectively recharge the aquifer. Due to the reduced recharge volume to the aquifer, the discharge from the stream is partially lower than the discharge from the epikarst during the early

https://doi.org/10.5194/egusphere-2025-324
Preprint. Discussion started: 17 February 2025

stage of the hydrological process.

With changes in precipitation intensity ($b = 3, 5,$ and 7), the water level variations and their differences between the karst aquifer and stream exhibit complex dynamic characteristics (Figs. 3d, 3e and 3f). During the early stage of precipitation, despite the increasing water level difference, the discharge from the stream to the aquifer is gradually decreasing (as shown by the negative values for PM I and PM II in Fig. 3a, 3b and 3c). This phenomenon indicates that water level is not the only factor controlling the interaction between the karst aquifer and stream; changes in the degree of saturation also play a significant role. As shown in Fig. 3d, under low precipitation intensity, the water level difference between the karst aquifer and stream is often greater than the water level of the stream during the middle and later stages of precipitation. However, as precipitation intensity increases, the water level difference tends to decrease (Fig. 3b and 3c). This change is primarily due to the increased precipitation intensity leading to a faster saturation of the karst aquifer, thereby limiting the ability of the stream to recharge the aquifer. After the middle stage of precipitation, the interaction between the stream and the upper part of the aquifer gradually intensifies, while the lower part of the aquifer discharges to the stream (Fig. 3a). Due to the gradual decrease in water level difference, it is difficult for the stream to effectively recharge the aquifer. In this process, the interaction between the aquifer and stream is controlled by the dynamic changes in saturation.

It is self-evident that changes in precipitation intensity significantly affect the

https://doi.org/10.5194/egusphere-2025-324
Preprint. Discussion started: 17 February 2025

recharge and discharge processes between the karst aquifer and stream. The water levels and saturation degrees of the respective media act as core controlling factors that jointly influence the interactive dynamics between the aquifer and stream. To gain a deeper understanding of these influencing factors and their interaction mechanisms, and to further elucidate the interaction process mechanisms between the karst aquifer and stream, this study focuses on the hydrological interaction process between the two during the early stage of precipitation.

3.2 Interaction process between the karst aquifer and stream during early stage of precipitation

Figure 4 illustrates how the interaction volume between the epikarst, porous media, and stream varies under different precipitation intensities. As shown in Fig. 4a, at a precipitation intensity $b = 3$, the contribution ratios of the epikarst, PM I, and PM II to the recharge of the stream are similar. This indicates that during the early stage of precipitation, the recharge effects of each medium on the stream are relatively balanced. Since groundwater vertically recharges the underlying aquifer through the epikarst, the discharge peak of PM II is relatively delayed compared to the epikarst and PM I.

As the precipitation intensity increases ($b = 5$), the contribution ratios of the epikarst, PM I, and PM II to the recharge of stream experience significant changes (Fig. 4b). Upon comparing Fig. 4a and 4b, it is evident that an increase in precipitation intensity leads to higher discharge volumes for both PM I and PM II, with PM II experiencing a more pronounced rise. Additionally, the peaks of their discharges occur

https://doi.org/10.5194/egusphere-2025-324
Preprint. Discussion started: 17 February 2025

earlier. The first peak of PM I is primarily caused by infiltration recharge from precipitation. With the increase in precipitation intensity, the infiltration velocity accelerates and the recharge volume increases, leading to a larger discharge volume and an earlier peak for PM I (vertical recharge peak). Groundwater continues to move downward from PM I, and the saturation of PM II rises, allowing more groundwater to overflow and discharge through PM I, thereby generating the second peak (overflow peak). For PM II, as discussed in Section 3.1, increase in saturation reduces the recharge from stream, but the discharge volume increases gradually after the middle stage of precipitation, and its contribution to the recharge of the stream becomes dominant among the three. This is due to the increased precipitation intensity, which allows PM II to receive more vertical recharge, enhancing its discharge capacity. When the precipitation intensity continues to increase ($b = 7$, Fig. 4c), PM II gradually reaches saturation. According to the analyses in Section 3.1, the ability of PM II to receive recharge is limited by its own saturation level, making it difficult to receive vertical recharge. Therefore, despite the increased precipitation intensity, the discharge volume of PM II does not increase significantly. Conversely, due to the influence of the saturation state of the underlying aquifer medium, the second peak (overflow peak) of PM I is more pronounced, indicating a more evident overflow phenomenon. Under higher precipitation intensity, the recharge contribution of PM I to the stream dominates.

Thus, variations in precipitation intensity notably influence the interaction volume between the karst media and stream. As precipitation intensity increases, the discharge

https://doi.org/10.5194/egusphere-2025-324
Preprint. Discussion started: 17 February 2025

volume and peak values of each medium are altered. Specifically, the two peaks of PM Ⅰ show sequential changes in intensity, which are modulated by the saturation levels of the adjacent media.

3.3 Impact of different water retention characteristics on the interaction process between the karst aquifer and stream

Figure 5 illustrates the changes in saturation of water retention curves based on two different retention equation for karst aquifer: the BC model (equations (12)-(13)) and the VGM model (equations (14)-(15)). For the same infiltration periods, the water content predicted by BC model is generally higher than that predicted by the VGM model. The BC model may focus more on the static retention of groundwater in the medium, while the VGM model may emphasize the dynamic transport and distribution of groundwater within the medium. Moreover, the VGM model predicts a greater distance of groundwater movement compared to the BC model, indicating that the VGM model may have higher sensitivity in simulating infiltration processes of groundwater in the medium. This difference is of significant importance for the dynamic process of unsaturated two-phase flow in the karst aquifer and for accurately predicting the advancement path of groundwater.

In addition, there are differences between the BC model and the VGM model in simulating the saturation changes of the water retention curve (Fig. 5). Not only do they differ in the degree of saturation change at the same time and location, but their simulation results for the distance of groundwater movement also vary. Therefore, it is

https://doi.org/10.5194/egusphere-2025-324
Preprint. Discussion started: 17 February 2025

crucial to select the appropriate model based on specific lithological conditions, as this can more accurately describe and predict the two-phase flow of karst groundwater.

The impact of different water retention models on the interaction process between the karst aquifer and stream is shown in Fig. 6. Compared to the BC model, the VGM model generally calculates lower discharge volumes from the stream. Therefore, under the simulation conditions of the VGM model, more groundwater is retained in the porous medium rather than being discharged through the stream. This reflects the differences between the two water retention models in simulating the movement and storage mechanisms of groundwater in the porous medium. During the early stage of precipitation recharge, the VGM model results show that the stream is more likely to recharge the karst conduit (Fig. 6b). Although the karst conduit receives more recharge from stream, their discharge to stream is relatively low. This indicates that the karst conduit derived from the VGM model receive relatively lower recharge intensities from the porous medium and sinkhole. As shown in Fig. 6c, due to the shorter distance of groundwater movement derived from the VGM model within the same time, the vertical infiltration capacity of the epikarst is reduced, thereby increasing the discharge volume of the epikarst to the stream. This indicates that the interaction process between stream and the epikarst is significantly influenced by the water retention characteristics. In the VGM model, the difficulty of groundwater moving vertically through the epikarst increases, leading to a decrease in the discharge volume of PM I (Fig. 6d). Since PM I receives limited recharge from the epikarst, its saturation remains at a low level, making

https://doi.org/10.5194/egusphere-2025-324
Preprint. Discussion started: 17 February 2025

it more favorable to receive recharge from stream (see Section 3.1).

The VGM model results suggest that the stream predominantly recharges PM II (as seen in Figs. 6e and 6c). However, during the middle and later stages, the stream recharge volume calculated by the BC model surpasses that of the VGM model. Figure 6f illustrates that the groundwater in the porous medium beneath the karst conduit primarily originates from conduit recharge. Meanwhile, Fig. 6b shows an increase in the discharge volume from the karst conduit, as estimated by the BC model. This increase subsequently affects the discharge volume of the porous medium below the karst conduit.

Therefore, different water retention models have a significant impact on the interaction process between the karst aquifer and stream. These impacts are not only reflected in the changes of discharge and recharge volumes but also involve the movement and storage mechanisms of groundwater in different media. In practical applications, selecting an appropriate water retention model based on the corresponding lithology can more accurately simulate and predict the interaction process between the karst aquifer and stream.

3.4 Impact of multi-stage permeability and porosity arrangement on the interaction process between the karst aquifer and stream

By comparing the effects of multi-level and single conduit arrangements on the interaction process, it is found that using multi-level and single conduit arrangements in underlying media does not cause significant changes in the hydrological processes

https://doi.org/10.5194/egusphere-2025-324
Preprint. Discussion started: 17 February 2025

of the epikarst and porous media (PM I and PM II, Fig. 7). As shown in Fig. 7a, when multi-level conduit arrangements are adopted, the peak of stream hydrological process increases, indicating that multi-level conduit arrangements enhance the recharge volume of stream. However, during the recession phase, the flow under multi-level conduit arrangements is relatively low. This is because multi-level conduit collects a proportion of the flow that should have been contributed by the later stage matrix recession and discharge it to stream, thereby affecting the peak of the recession process. As shown in Fig. 7b, under multi-level conduit arrangements, sinkhole can absorb more water and discharge it through karst conduit. This indicates that multi-level conduit arrangements can more effectively play their roles in water absorption and discharge during heavy precipitation events. However, in the case of lower precipitation intensity in the early stage, the water absorption priority of multi-level conduit is not fully manifested. By comparing Figs. 7c, 7d, and 7e, it is found that multi-level conduit arrangements have no significant impact on the hydrological processes of the epikarst and porous media (PM I and PM II). This suggests that multi-level conduit arrangements mainly affect the interaction between the karst conduit and stream, with relatively little impact on other media. The hydrological responses of the karst conduit and PM II under multi-level conduit arrangements are shown in Figs. 7f and 7b. Under multi-level conduit arrangements, the discharge volume of the karst conduit significantly increases. At the same time, due to the increase in karst conduit flow, PM II also receives more recharge, leading to a corresponding increase in the discharge

https://doi.org/10.5194/egusphere-2025-324
Preprint. Discussion started: 17 February 2025

volume of this portion of porous media to stream. This further indicates that multi-level conduit configurations can notably influence the hydrological processes of stream and karst conduit under specific precipitation intensities, with minimal effects on other media.

3.5 Impact of multiple precipitation events on the interaction process between the karst aquifer and stream

Rainy seasons typically experience multiple precipitation events, during which differences in precipitation peaks, durations, and cumulative precipitation events can all impact the interaction process between the karst aquifer and stream. Based on understanding the interaction mechanism of a single precipitation event, this study further analyzes the impact of multiple precipitation events on the interaction process. Figure 8 shows the changes in water level of stream under continuous precipitation events. When the intensities of two consecutive precipitation events remain constant, the water level of stream reaches both the highest and the lowest points, indicating that the water level is related to the total precipitation intensity. Even with different intensities of the first precipitation event (b_1 =3 and b_1 =5), the trend of the water level changes in stream is consistent (Fig. 8① and ④). After the first precipitation event, the karst aquifer receives infiltration recharge from the precipitation and can store part of the water, so the water level of stream will be higher during the second precipitation event, and the greater the intensity of the second precipitation event, the higher the water level of stream (Fig. 8① and ②, or ③ and ④). This indicates that the intensity

https://doi.org/10.5194/egusphere-2025-324
Preprint. Discussion started: 17 February 2025

of the second precipitation event determines the amount of recharge from each medium to stream. Therefore, when the intensity of the first precipitation event is the same, the amplitude of the water level change in stream during the second precipitation event is only related to the intensity of the second precipitation event. When the intensity of the second precipitation event is the same, the storage capacity of the karst aquifer during the first precipitation event determines the amplitude of the water level change in stream during the second precipitation event. When the total precipitation intensity is the same (Fig. 8 ② and ③), if the intensity of the first precipitation event is lower than that of the second one, the amplitude of the water level change in stream is higher, and vice versa. This is because, in the case of two consecutive precipitation events, part of the precipitation infiltrates and recharge the storage during the first event, and the other part is discharged to stream through the aquifer. Combining Fig. 3d and 3e, during the first precipitation event, the water level in the porous medium rises and stores a proportion of water, but the discharge volume to stream is greater when the precipitation intensity is higher ($b_1 = 5$) compared to when it is lower ($b_1 = 3$, Fig. 3a and b). When the second precipitation event occurs, due to the similar saturation levels of the karst aquifer, the greater the intensity of the second precipitation event, the larger the amount of groundwater recharged to stream through the aquifer, and the more pronounced the amplitude of the water level in stream.

Figure 9 illustrates the hydrological process curves of the stream during two consecutive precipitation events, as well as the interaction processes between the

https://doi.org/10.5194/egusphere-2025-324
Preprint. Discussion started: 17 February 2025

various media of the karst aquifer and stream. Under different precipitation intensities, the various media of the karst aquifer recharge the stream with varying intensities, resulting in significant fluctuations in the water level of stream. Combining Fig. 9a and Fig. 8 (② and ④), it can be concluded that during two consecutive precipitation events, when the intensity of the second precipitation is greater than or equal to that of the first one, the amplitude of the hydrological process of stream is larger. As shown in Fig. 9b, the epikarst discharges quickly and is not easily affected by multiple precipitation events. However, when the intensity of the first precipitation is high and the intensity of the second precipitation is the same (① and ③), the discharge volume of the epikarst to stream during the second precipitation period is slightly larger. When the intensity of the first precipitation is different and the intensity of the second precipitation is the same (Fig. 9c ② and ④), the discharge volume of groundwater through karst conduit to stream during the second precipitation period is almost the same. This is because karst conduit discharge quickly, and the storage volume of the conduit during the first precipitation period has little impact on the storage volume during the second precipitation period. Therefore, combining with Fig. 8, it is known that the storage effect of the karst aquifer mainly occurs in the porous medium, and it also indicates that relying solely on changes in the water level of stream makes it difficult to clearly determine the storage volume of the porous medium and conduit during the first precipitation event, and their respective impacts on the second precipitation period (Fig. 8). When the intensity of the second precipitation is higher (Fig. 9c ②, ③ and ④), the

https://doi.org/10.5194/egusphere-2025-324
Preprint. Discussion started: 17 February 2025

discharge volume of the porous medium (PM II) to stream does not increase significantly. This is because the intensity of the second precipitation is larger, causing the water level of stream to rise (Fig. 8), making it difficult for the porous medium (PM II) to recharge stream.

Therefore, under the influence of two consecutive precipitation events, the greater the total precipitation intensity, the larger the discharge volume of the karst aquifer to stream. The storage effect of the karst aquifer occurs in the porous medium and affects subsequent precipitation processes. The lower-level porous medium (PM II), due to the high water level and large fluctuations of stream, is more difficult to recharge stream, and the recharge from stream mostly comes from overflow supply from the media in other layers.

4. Discussion

4.1 Comparison with the simulation results of MODFLOW-CFP

To better assess the applicability of the Darcy-Brinkman-Stokes model in simulating the interaction between the karst aquifer and stream, this study compares its simulation outcomes with those from MODFLOW-CFP. As depicted in Fig. 10(a.1), the study contrasts the coupling approaches of conduits and porous media in both MODFLOW-CFP and the Darcy-Brinkman-Stokes model, focusing on control equations and grid discretization. In the MODFLOW-CFP model, the groundwater flow during the interaction process is determined by the stable water levels between the conduit-porous media and stream-porous media interfaces (Fig. 10(a.2)). In the Darcy-

https://doi.org/10.5194/egusphere-2025-324
Preprint. Discussion started: 17 February 2025

Brinkman-Stokes model, however, the groundwater interaction among the conduit, the stream, and the porous media depends on the saturation and pressure differences between adjacent grid points. It allows the groundwater interaction among the conduit, the stream, and the porous media to be recharged or discharged simultaneously at different positions. However, this also requires calculating the changes in all grid fluxes (Fig. 10(a.3)).

This study further compares the interaction modes between the stream and porous media in MODFLOW-CFP and Darcy-Brinkman-Stokes. In MODFLOW-CFP, the stream is discretized among single grid cells. The interaction volume between the stream and porous media depends on the water level difference between them. The fluctuating water surface of the stream is generalized to a unified water level value, and the "dry area" cannot be simulated in the porous media area (as shown in Fig. 10(a.4)). In Darcy-Brinkman-Stokes, the modeling of each medium is completed by specifying the specific porosity and permeability at each grid node. At the interface, the values are interpolated to the average grid cell value based on the values between nodes. Therefore, the interaction interface where the conduit is directly connected to the stream does not need the porous media as an intermediate. On this basis, the shape of the stream can be established as a regular rectangle or an irregular channel. The Darcy-Brinkman-Stokes simulates the free flow by reconstructing the water-vapor interface tracer through the VOF (Volume of Fluid) and Front-tracking methods. Therefore, when the grid is fine enough, it can simulate the fluctuating water-vapor interface (as shown in Fig. 10(a.5)).

https://doi.org/10.5194/egusphere-2025-324
Preprint. Discussion started: 17 February 2025

This study further reveals the interaction mode of groundwater between the conduit and stream in the Darcy-Brinkman-Stokes model and the differences from the simulation results of MODFLOW-CFP through a generalized karst aquifer. As shown in Fig. 11, the karst conduit is surrounded by porous media and are directly connected to the stream. The aquifer is 200 m long, 200 m wide, and 30 m thick. As shown in Fig. 11(a.1), groundwater is replenished from the porous media to the conduit and discharged into the stream. The model parameters are as follows: assume that the porous media is a homogeneous medium with a hydraulic conductivity of 0.65 m/s. The interaction parameter of the conduit wall is 25 m/s, the conduit diameter is 1 m, the conduit roughness is 0.01 m, and the conduit outlet and the stream are in the same grid cell, and the interaction is simulated through the porous media. The initial spring flow is set to zero, the initial head of the porous media is also set to 10 m, and the vertical height of the conduit node is 1 m. The groundwater temperature in the conduit is set to 20 °C, and the surrounding boundaries are no-flow boundaries. The upper boundary is a rainfall boundary (Equation 16), where $b = 5$. According to Huang et al. (2024), μ, σ^2, and a are set as constants (90, 1.5, and 20) respectively. The total simulation period is 25000 s. In the MODFLOW-CFP model, each stress period is set to 1 minute, and in the Darcy-Brinkman-Stokes model, due to the Courant number limitation, each time step is less than 0.1 s.

Through a comparative analysis of the simulations of MODFLOW-CFP and Darcy-Brinkman-Stokes (the simulated hydrograph of the stream in the Darcy-

https://doi.org/10.5194/egusphere-2025-324
Preprint. Discussion started: 17 February 2025

Brinkman-Stokes model in Fig. 3(b)), as shown in Fig. 11(a.2), there are three differences in the simulation results between the MODFLOW-CFP model and the Darcy-Brinkman-Stokes model: (1) The hydrograph of the stream in the MODFLOW-CFP model lags behind the Darcy-Brinkman-Stokes model in terms of rising. This is because in the Darcy-Brinkman-Stokes model, the rapid lateral runoff of epikarst causes the hydrograph of the stream to rise rapidly. (2) The peak discharge of the Darcy-Brinkman-Stokes model is slightly lower. This is because a part of the storage capacity of the porous medium has been drained by the rapid lateral runoff of epikarst. By using the rainfall directly infiltrating into the stream (P -River) to represent the time nodes of the rainfall peak and comparing it with the time nodes of the peak discharge of the stream simulated by MODFLOW-CFP and Darcy-Brinkman-Stokes, it is found that both MODFLOW-CFP and Darcy-Brinkman-Stokes exhibit a lag of 2000 s in the rainfall peak. (3) In the Darcy-Brinkman-Stokes model, the rapid lateral runoff of epikarst reduces the storage capacity of the upper porous medium. Therefore, during the initial base flow recession stage, the discharge of the stream in the Darcy-Brinkman-Stokes model is lower than the simulated value of MODFLOW-CFP. As the storage capacity of the porous medium gradually decreases, the influence of epikarst gradually weakens, and the recession amounts of the two tend to be the same.

4.2 Dynamic interaction processes among various media

Through a comparative analysis of the hydrographs of the stream simulated by MODFLOW-CFP model and the Darcy-Brinkman-Stokes model, it is found that the

https://doi.org/10.5194/egusphere-2025-324
Preprint. Discussion started: 17 February 2025

two models have similar effects in simulating the interaction between the karst aquifer and stream under rainfall infiltration recharge. However, with its fine grid and two-phase flow simulation capabilities, the Darcy-Brinkman-Stokes model can accurately capture the interaction processes among various media, such as between the saturated and unsaturated zones at various stages under the influence of the dynamic saturation process, and between the conduit and the stream, under rainfall infiltration recharge.

As shown in Fig. 12, the Darcy-Brinkman-Stokes model clearly demonstrates the changes in the saturation levels of epikarst, porous media, and the karst spring; the saturation fields and the interaction between various media at 4000 s, 6105 s, and 7363 s; the interaction amounts between epikarst, porous media I, II, III, and the stream. From Fig. 12 (a.1), it can be seen that the saturation level of epikarst rises and declines earliest, but the saturation level is relatively low, and it is in a completely unsaturated flow state. Porous media I and III rise synchronously before 5000 s, while porous media II and the karst spring rise rapidly at 4611 s. At 7409 s, the karst spring and porous media I successively enter the decline stage. Due to the rapid drainage of the conduit, the saturation level decreases. The saturation level of the karst spring decreases faster than that of porous media I and intersects with porous media I at 9670 s.

Combining Fig. 12 (a.2) with other sub-figures, the stages with obvious interactions among porous media can be divided into the infiltration stage (green), the overflow stage (red), and the recession stage (blue). During the infiltration stage from 4000 s to 4611 s, as shown in Fig. 12 (a.2.1), epikarst vertically replenishes porous

https://doi.org/10.5194/egusphere-2025-324
Preprint. Discussion started: 17 February 2025

medium I and infiltrates downward. However, the infiltrating water does not reach the lower media. Meanwhile, the saturation levels of porous media II, III, and the conduit gradually increase (see Fig. 12 (a.1)). Combining with Fig. 12 (a.3), it can be seen that epikarst laterally replenishes the stream, and quickly drops to the bottom of the riverbed due to gravity. At this time, the lower aquifer system (porous media II, III, and the conduit) is in a dry state, so the stream replenishes the lower aquifer. The amount of recharge received by porous medium III and the conduit is less than that of porous medium II (analyzed by combining Fig. 12 (a.3) and (a.4)), but their saturation levels increase faster. There are two reasons for this situation: First, the bottom elevation of the conduit is 1 m, and the water level of the stream needs to submerge the 1 m water level before it can recharge the conduit. Second, porous medium III is not only replenished by the stream, but also the sinkhole diverts the groundwater in epikarst and porous medium I to the conduit (the sinkhole flow velocity and saturation as shown in Fig. 12 (a.2.1)), and then replenishes porous medium III. As the lower aquifer media gradually tends to be saturated with rainfall recharge, as shown in Fig. 12 (a.2.2), porous media II and III tend to be saturated (see Fig. 12 (a.2.1)). Due to the weak compressibility of water, after the upper part infiltrates and replenishes porous medium I, it tends to laterally replenish the stream from the interface between porous medium II and stream. As the saturation level of porous medium I gets higher, the lateral recharge to the stream becomes more significant, showing an obvious overflow state. The depression between the two peaks is caused by the rapid rise of the stream water

https://doi.org/10.5194/egusphere-2025-324
Preprint. Discussion started: 17 February 2025

level. During the flood peak stage, the discharge from porous media to stream decreases. At the same time, the rise of the stream water level makes it difficult for the lower porous media to replenish the stream, and porous medium II tends to be saturated, making it difficult to replenish porous medium I. During this stage, the flow between porous media I and II is in a dynamic equilibrium state. As shown in Fig. 12 (a.2.3), during the recession stage, the rainfall infiltration intensity decreases rapidly. Under the action of gravity, the groundwater vertically replenishes porous medium I, the conduit, and porous medium II successively recedes. And the water level of the stream drops rapidly (see Fig. 3 (e)). The groundwater tends to be discharged to the stream through porous medium I and the karst spring. Porous medium I is replenished by porous medium II on the one hand and discharges to the stream on the other hand. Therefore, during a single rainfall event, during the infiltration stage, part of the amount of water replenished from epikarst to the stream is discharged, and other part is redirected to replenish the lower porous media; during the overflow stage, the stream is mainly replenished through the karst conduit and porous medium II. Porous medium I and the stream are in a dynamic equilibrium state. During the recession stage, the porous media act as the main medium to replenish the stream.

As shown in Fig. 12 (a.4), the karst spring reaches its peak at 7409 s. This is due to the rainfall infiltration, the recharge from porous medium I, and the subsequent discharge to the stream. As the storage volume decreases, the amount of recharge from the karst spring to the stream decreases. A trough appears at 11642 s. This is because

https://doi.org/10.5194/egusphere-2025-324
Preprint. Discussion started: 17 February 2025

as the water level of the stream drops, groundwater is more easily discharged into the stream. However, as the overall storage volume continues to decline, after a peak appears at 13057 s, it enters a complete recession stage. Affected by the decline of the stream water level, the discharge from porous medium III to the stream gradually increases during the recession stage. Combining with Fig. 12 (a.1), it can be seen that while porous medium III is discharging, its saturation remains at level I continuously, indicating that the conduit continuously supplies water vertically to porous medium III.

Under the recharge of rainfall infiltration, the interaction process between the karst aquifer affected by epikarst, sinkholes, conduit and the stream shows dynamic changes in terms of staged characteristics, main interaction media, and the dynamic equilibrium process among different media. The accurate simulation of the above complex processes depends on the support of a three-dimensional two-phase numerical model (Darcy-Brinkman-Stokes model).

5. Conclusions

This study employed the Darcy-Brinkman-Stokes equation to characterize groundwater flow in the karst aquifer and stream, as well as within the karst media. The VOF phase change method was used to illustrate the two-phase flow of water and air in porous media, while various water retention models were applied to describe the unsaturated flow processes in the karst aquifer. The results indicate that changes in precipitation intensity have a significant impact on the interaction between the karst aquifer and stream. As the precipitation intensity increases, the interaction process

https://doi.org/10.5194/egusphere-2025-324
Preprint. Discussion started: 17 February 2025

between the two becomes more complex, involving multi-media synergistic recharge and dynamic interaction with the karst aquifer. The contribution ratios of the epikarst, upper layer, and PM II to the stream change with increasing precipitation intensity. In the early stages of precipitation, the recharge effects of each medium on the stream are relatively balanced; as the precipitation intensity increases, the discharge volumes of PM I and PM II both increase, especially the increase in PM II is more significant, and the timing of its discharge peak advances; when the precipitation intensity further increases, PM II gradually reaches saturation, limiting its discharge capacity; and during this process, the double peak intensity of PM I changes with the precipitation intensity; at the same time, due to the saturation of PM II, a more pronounced overflow phenomenon occurs in PM I, which dominates the contribution of recharge volume to the stream. Therefore, the change in precipitation intensity not only affects the discharge volume and discharge peak of each medium in the karst aquifer but also is influenced by the dynamic saturation process of adjacent media.

The impact of different water retention models on the hydrological processes of the stream and various media is also quite significant. The VGM model leads to more water being retained in the porous media, thereby reducing the discharge volume of the stream. In the early stage of precipitation, the VGM model enhances the recharge effect of the stream on the karst conduit, but the discharge volume of the karst conduit to the stream is relatively low in the middle and later stages. Additionally, the VGM model predicts shorter movement distances of karst groundwater, weakening the vertical

https://doi.org/10.5194/egusphere-2025-324
Preprint. Discussion started: 17 February 2025

infiltration capacity of the epikarst, resulting in an increase in the discharge volume of the epikarst to the stream. At the same time, based on the VGM model, the discharge volume of PM I decreases, but due to the smaller recharge volume, lower saturation level, and water level, the stream is more likely to recharge it. The porous media located below the karst conduit mainly rely on the recharge from the conduit, and based on the BC model, the discharge volume of the karst conduit is larger. Ultimately, based on the VGM model, it is found that the stream is more likely to recharge PM II in the early stage of precipitation; in the middle to late stages of precipitation, the discharge volume predicted by the BC model exceeds that of the VGM model.

During heavy precipitation events, multi-level conduit arrangements can significantly impact the interaction process between the karst aquifer and stream, and exhibit higher discharge efficiency. However, this arrangement has relatively little impact on other media, indicating that multi-level conduit arrangements primarily influence the hydrological process by regulating the interaction between the karst conduit and stream.

For two consecutive precipitation events, the total precipitation intensity directly affects the changes in water level of stream. Different precipitation intensities result in different trends of water level changes in stream. The porous media of the karst aquifer store a proportion of groundwater during the first precipitation period, which affects the water level changes of stream during the second precipitation period. Due to the rapid discharge characteristics of the karst conduit, the storage volume of the conduit during

https://doi.org/10.5194/egusphere-2025-324
Preprint. Discussion started: 17 February 2025

the first precipitation period has little impact on the storage volume during the second precipitation period. When the intensity of the first precipitation is higher than that of the second, the amplitude of water level changes in stream is smaller, and vice versa. The changes in water level of stream can affect the ease of recharge from different layer media of the karst aquifer to the stream.

Through the generalized karst aquifer, the interaction mode of groundwater between the conduit and stream in the Darcy-Brinkman-Stokes model and the differences from the simulation results of MODFLOW-CFP were further revealed. Moreover, a comparative analysis of the two types of models was carried out through the hydrograph of the stream. The results show that the Darcy-Brinkman-Stokes model can effectively simulate the interaction process between the karst aquifer and stream under the influence of rainfall, and refine the two-phase interactive flow among various media affected by the dynamic saturation process. At the same time, the Darcy-Brinkman-Stokes model can represent the dynamic interaction process affected by epikarst, sinkholes, conduit and the stream under the recharge of rainfall infiltration, and refine and explain the significant infiltration process, overflow process and recession process.

Acknowledgments

This research was partially funded by the Doctoral Scientific Research Startup Foundation of Xinjiang University grant 620321004, and the Natural Science Foundation of Xinjiang Uygur Autonomous Region grant 2022D01C40.

Data availability. All raw data can be provided by the corresponding author upon request.

Author contributions. **FH**: conceptualization, methodology, formal analysis, visualization, writing original draft. **YG**: conceptualization, methodology, formal analysis, visualization, review and editing. **XH**: visualization, review and editing. **XW**: methodology, review and editing. **SP**: writing original draft and review and editing.

Competing interests. The authors declare that they have no conflict of interest.

References

Z. Li, X. Xu, M. Liu, et al.State-space prediction of spring discharge in a karst catchment in Southwest ChinaJ. Hydrol., 549 (2017), pp. 264-276, 10.1016/j.jhydrol.2017.04.001

Ford, D., & Williams, P. (2007). Karst hydrogeology and geomorphology. West Sussex, England: John Wiley & Sons Ltd. https://doi.org/10.1002/9781118684986

V. Sivelle, H. Jourde, D. Bittner, N. Mazzilli, Y. Tramblay.Assessment of the relative impacts of climate changes and anthropogenic forcing on spring discharge of a Mediterranean karst system. J. Hydrol., 598 (2021), Article 126396, 10.1016/j.jhydrol.2021.126396

https://doi.org/10.5194/egusphere-2025-324
Preprint. Discussion started: 17 February 2025

J. Longenecker, T. Bechtel, Z. Chen, et al. Correlating global precipitation measurement satellite data with karst spring hydrographs for rapid catchment delineation. Geophys. Res. Lett., 44 (10) (2017), pp. 4926-4932, 10.1002/2017gl073790

Goldscheider, N., Chen, Z., Auler, A.S., Bakalowicz, M., Broda, S., Drew, D., Hartmann, J., Jiang, G., Moosdorf, N., Stevanovic, Z., Veni, G., 2020. Global distribution of carbonate rocks and karst water resources. Hydrgeol. J. 28 (5), 1661–1677.

B.J. Mahler, Y. Jiang, J. Pu, J.B. Martin. Editorial: advances in hydrology and the water environment in the karst critical zone under the impacts of climate change and anthropogenic activities. J. Hydrol., 595 (2021), Article 125982, 10.1016/j.jhydrol.2021.125982

Kuniansky, E.L., 2016. Simulating groundwater flow in karst aquifers with distributed parameter models— Comparison of porous-equivalent media and hybrid flow approaches: U.S. Geological Survey Scientific Investigations Report 2016–5116, pp. 14. doi:https://doi.org/10.3133/sir20165116

L. Zhang, M. Luo, Z. Chen. Identification and estimation of solute storage and release in Karst water systems, south China. Int. J. Environ. Res. Public Health, 17 (2020), pp. 1-13, 10.3390/ijerph17197219

Bonacci,O., 2015. Surface Waters and Groundwater in Karst. Z. Stevanović (ed.), Karst Aquifers – Characterization and Engineering, Professional Practice in Earth Science. Springer International Publishing Switzerland.153-155.

F. Guo, G. Jiang. Hydro-ecological processes of hyporheic zone in a karst spring-fed p

https://doi.org/10.5194/egusphere-2025-324
Preprint. Discussion started: 17 February 2025

ool: Effects of groundwater decline and river backflow. J. Hydrol., 587 (2020), Article 124987, 10.1016/j.jhydrol.2020.124987

Gao, Y., Yao, L., Chang, N.-B., and Wang, D.: Diagnosis toward predicting mean annual runoff in ungauged basins, Hydrol. Earth Syst. Sci., 25, 945–956, https://doi.org/10.5194/hess-25-945-2021, 2021.

E. Lee, N. Krothe. A four-component mixing model for water in a karst terrain in south-central Indiana, USA. Using solute concentration and stable isotopes as tracers. Chem. Geol., 179 (2001), pp. 129-143

A.M.L.S. Okello, S. Uhlenbrook, G.P.W. Jewitt, I. Masih, E.S. Riddell, V.D.Z. Pieter. Hydrograph separation using tracers and digital filters to quantify runoff components in a semi-arid mesoscale catchment. Hydrol. Process., 32 (10) (2018), pp. 1334-1350

L. Duran, N. Massei, N. Lecoq, M. Fournier, D. Labat Analyzing multi-scale hydrodynamic processes in karst with a coupled conceptual modeling and signal decomposition approach J. Hydrol., 583 (2020), Article 124625, 10.1016/j.jhydrol.2020.124625.

Bittner, D., Parente, M. T., Mattis, S., Wohlmuth, B., & Chiogna, G. (2020). Identifying relevant hydrological and catchment properties in active subspaces: An inference study of a lumped karst aquifer model. Advances in Water Resources, 135, 103472. https://doi.org/10.1016/j.advwatres.2019.103472

S. Bianchini, P. Confuorto, E. Intrieri, P. Sbarra, D. Di Martire, D. Calcaterra, R. Fanti.

https://doi.org/10.5194/egusphere-2025-324
Preprint. Discussion started: 17 February 2025

Machine learning for sinkhole risk mapping in Guidonia-Bagni di Tivoli plain (Rome). Italy. Geocarto International, 37 (27) (2022), pp. 16687-16715

Halihan, T., R.E. Mace, and J.M. Sharp Jr., 1999. Interpreting flow using permeability at multiple scales. Karst Modeling, Special Publication, 5.

Worthington, S. R. (1991), Karst Hydrogeology of the Canadian Rocky Mountains, 227 pp., McMaster Univ., Hamilton, Ont., Canada.

Huang, F., Gao, Y., Hu, X., Wang, X., & Pu, S. (2024). Influence of precipitation infiltration recharge on hydrological processes of the karst aquifer system and adjacent river. *Journal of Hydrology*, 639, 131656. https://doi.org/10.1016/j.jhydrol.2024.131656

Shoemaker, W. B., E. L. Kuniansky, S. Birk, S. Bauer, and E. D. Swain (2008), Documentation of a Conduit Flow Process (CFP) for MODFLOW-2005, US Department of the Interior, US Geological Survey, Reston, Va.

A. Kavousi, T. Reimann, R. Liedl, E. Raeisi Karst aquifer characterization by inverse application of MODFLOW-2005 CFPv2 discrete-continuum flow and transport model. J. Hydrol., 587 (2020), 10.1016/j.jhydrol.2020.124922

H. Qiu, J. Niu, B.X. Hu Quantifying the integrated water and carbon cycle in a data-limited karst basin using a process-based hydrologic model Environ. Earth Sci., 78 (11) (2019), p. 328

Gao, Y., Libera, D., Kibler, K., Wang, D*., Chang, N.B., 2020. Evaluating the performance of BAM-based blanket filter on nitrate reduction in a karst spring. Journal of

https://doi.org/10.5194/egusphere-2025-324
Preprint. Discussion started: 17 February 2025

Hydrology, 591, 125491. Doi: 10.1016/j.jhydrol.2020.125491.

Gao, Y., Huang, F., Wang, D. Evaluating physical controls on conduit flow contribution to spring discharge. Journal of Hydrology, 2024. Doi:10.1016/j.jhydrol.2024.130754.

Soulaine, C., Tchelepi, H.A. Micro-continuum Approach for Pore-Scale Simulation of Subsurface Processes. Transp Porous Med 113, 431–456 (2016). https://doi.org/10.1007/s11242-016-0701-3

Nillama L.B.A., Yang J., Yang L.An explicit stabilised finite element method for Navier-Stokes-Brinkman equationsJ. Comput. Phys., 457 (2022), Article 111033, 10.1016/j.jcp.2022.111033

F.J. Carrillo, I.C. Bourg, C. Soulaine. Multiphase flow modeling in multiscale porous media: An open-source micro-continuum approach J. Computat. Phys.: X, 8 (2020), Article 100073, 10.1016/j.jcpx.2020.100073

Yanyan Zhai, David R. Fuhrman, Erik Damgaard Christensen,Numerical simulations of flow inside a stone protection layer with a modified k-ω turbulence model,Coastal Engineering,Volume 189,2024,104469,ISSN 0378-3839,https://doi.org/10.1016/j.coastaleng.2024.104469.

A. Nahlieli, T. Svoray, E. Argaman. Piping formation and distribution in the semi-arid Northern Negev environment: a new conceptual model. Catena, 213 (2022), Article 106201, 10.1016/j.catena.2022.106201

S.-F. Lu, Y.-X. Wang, M.-Y. Ma, L. Xu. Water seepage characteristics in porous media

https://doi.org/10.5194/egusphere-2025-324
Preprint. Discussion started: 17 February 2025

with various conduits: Insights from a multi-scale Darcy-Brinkman-Stokes approach. Computers and Geotechnics, 157 (2023), p. 105317

Soulaine, C. (2024). Micro-continuum modeling: An hybrid-scale approach for solving coupled processes in porous media. *Water Resources Research*, 60, e2023WR035908. https://doi.org/10.1029/2023WR035908.

T. Reimann, C. Rehrl, W.B. Shoemaker, T. Geyer, S. BirkThe significance of turbulent flow representation in single-continuum models Water Resour. Res., 47 (9) (2011), p. W09503

del Jesus, M., Lara, J.L., Losada, I.J., 2012. Three-dimensional interaction of waves and porous coastal structures: Part I: numerical model formulation. Coast. Eng. 64, 57–72. https://doi.org/10.1016/j.coastaleng.2012.01.008.

Higuera, P., Lara, J.L., Losada, I.J., 2014. Three-dimensional interaction of waves and porous coastal structures using OpenFOAM®. Part I: formulation and validation. Coast. Eng. 83, 243–258. https://doi.org/10.1016/j.coastaleng.2013.08.010.

R. Brooks, A. Corey, Hydraulic properties of porous media, Hydro Paper 3, Colorado State University, 1964, p. 27.

Kuang, X., and J. J. Jiao (2011), A new model for predicting relative nonwetting phase permeability from soil water retention curves, Water Resources Research, 47, W08520, doi:10.1029/2011WR010728.

Parker, J. C., Lenhard, R. J., & Kuppusamy, T. (1987). A parametric model for constitu

https://doi.org/10.5194/egusphere-2025-324
Preprint. Discussion started: 17 February 2025

tive properties governing multiphase flow in porous media. Water Resources Research, 23(4), 618–624.

Y. Chang, J. Wu, L. Liu Effects of the conduit network on the spring hydrograph of the karst aquifer J. Hydrol., 527 (2015), pp. 517-530.

Li, Y.X., Shu, L.C., Wu, P.P., Zou, Z., Lu, C.P., Liu, B., Niu, S.Y., Yin, X.R., 2023. Influence of the karst matrix hydraulic conductivity and specific yield on the estimation accuracy of karstic water storage variation. J. Hydrol. 626 (Part A) https://doi.org/10.1016/j.jhydrol.2023.130186. ISSN 0022-1694.

https://doi.org/10.5194/egusphere-2025-324
Preprint. Discussion started: 17 February 2025

887 Table 1: Different parameter used in the models

Parameters	Units	Value
Conduit radius r_c	m	0.5
Secondary Conduit radius r_{c2}	m	1
Tertiary Conduit radius r_{c3}	m	1.5
Sinkhole radius r_s	m	0.5
Secondary Sinkhole radius r_{s2}	m	1
Tertiary Sinkhole radius r_{s3}	m	2
Level IV Sinkhole radius r_{s4}	m	5
Conduit height h_S	m	2
River width L_r	m	2
EpiKarst thickness	m	4
Porous medium I thickness	m	13
Porous medium II thickness	m	3
Porous medium III thickness	m	1
Porous medium length L_{py}	m	200
Porous media width L_{px}	m	200
Gravity g	m/s^2	9.81
Porous medium Porosity φ	/	0.4
Secondary permeability coefficient k_{02}	m^2	10^{-6}
Tertiary permeability coefficient k_{03}	m^2	10^{-7}
Level IV permeability coefficient k_{04}	m^2	10^{-8}
Porous medium Permeability coefficient k_0	m^2	10^{-9}
Gas phase viscosity μ_a	m^2/s	$1.48*10^{-5}$
Gas phase density ρ_a	Kg/m^3	1.29
Liquid phase viscosity μ_w	m^2/s	10^{-6}
Liquid phase density ρ_w	Kg/m^3	10^3
m (Van Genuchten)	/	0.75
m (Brooks and Corey)	/	3
Precipitation Intensity b	m	3-7

888

https://doi.org/10.5194/egusphere-2025-324
Preprint. Discussion started: 17 February 2025

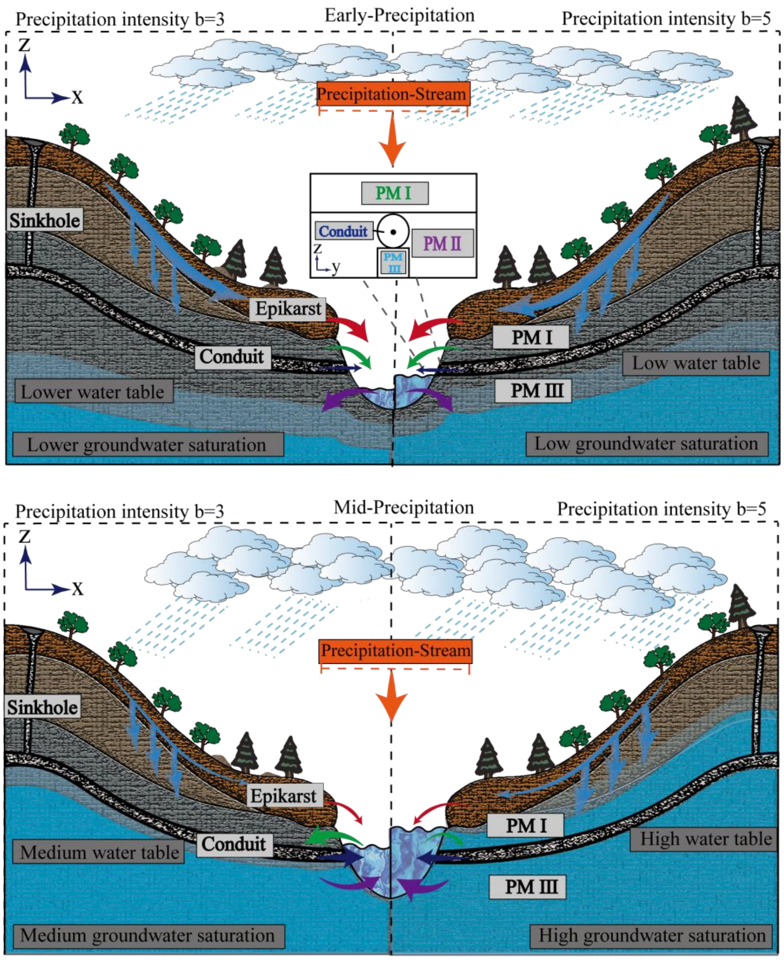

Figure 1. Schematic diagrams of the modelling of the interaction between the karst aquifer (epikarst, sinkhole, karst conduit, PM I, PM II, and PM III) and stream under dimensionless precipitation intensities (b = 3 and b = 5). (a) Schematic diagram of the interaction flow between each medium and stream in the early stage of a precipitation event; (b) Schematic diagram of the interaction flow between each medium and stream in the middle stage of a precipitation event. The size of the arrows represents the magnitude of the flow rate, and the direction of the arrows represents the direction of interaction between the two.

https://doi.org/10.5194/egusphere-2025-324
Preprint. Discussion started: 17 February 2025

897 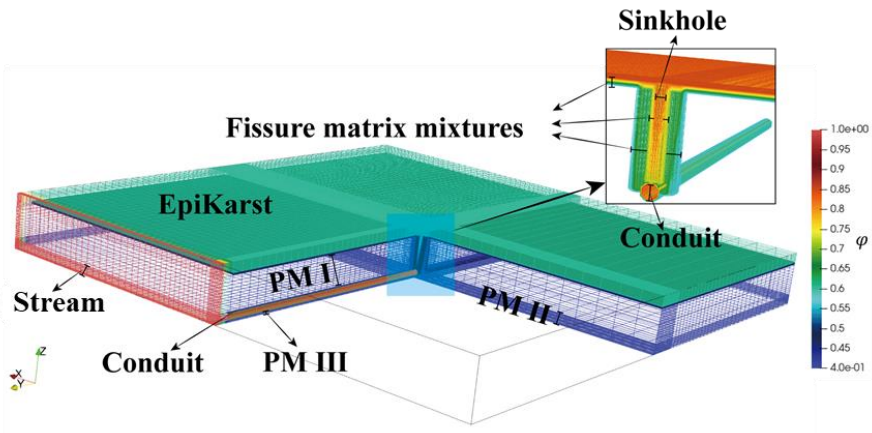

898 Figure 2. Discrete scheme for the karst aquifer and stream model.

https://doi.org/10.5194/egusphere-2025-324
Preprint. Discussion started: 17 February 2025

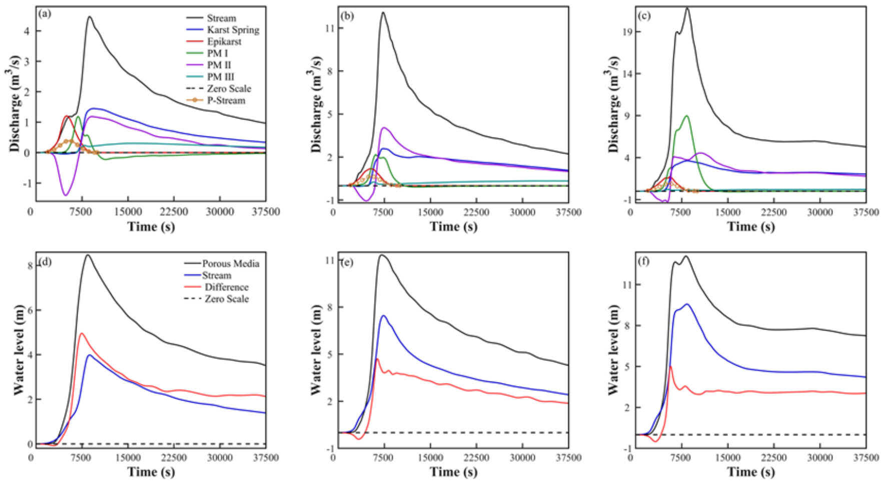

Figure 3. Hydrological process curves of each medium in the karst aquifer and stream for different precipitation intensities: (a) $b = 3$, (b) $b = 5$, (c) $b = 7$. Water level changes and differences in water levels in the karst aquifer and stream for different precipitation intensities: (d) $b = 3$, (e) $b = 5$, (f) $b = 7$.

https://doi.org/10.5194/egusphere-2025-324
Preprint. Discussion started: 17 February 2025

905 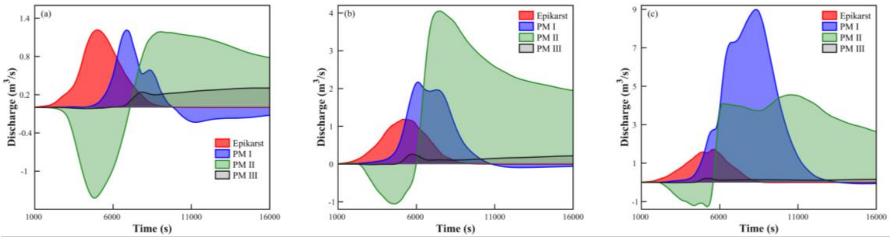

906 Figure 4. Interaction process of epikarst, porous media, and stream for different precipitation
907 intensities: (a) $b = 3$, (b) $b = 5$, (c) $b = 7$.

https://doi.org/10.5194/egusphere-2025-324
Preprint. Discussion started: 17 February 2025

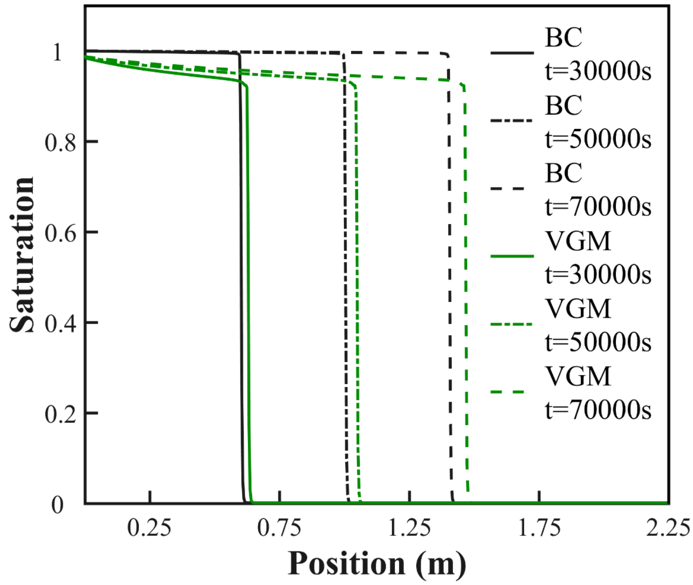

908
909 Figure 5. Water retention curves obtained using BC and VGMM water retention equations.

https://doi.org/10.5194/egusphere-2025-324
Preprint. Discussion started: 17 February 2025

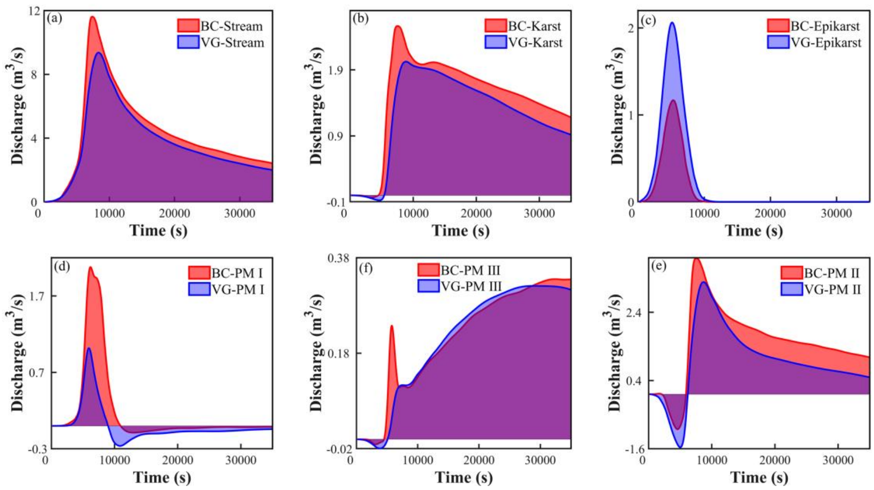

Figure 6. Changes in hydrological processes in the media of the karst aquifer derived from BC and VGMM water retention equations for a precipitation intensity $b = 5$.

https://doi.org/10.5194/egusphere-2025-324
Preprint. Discussion started: 17 February 2025

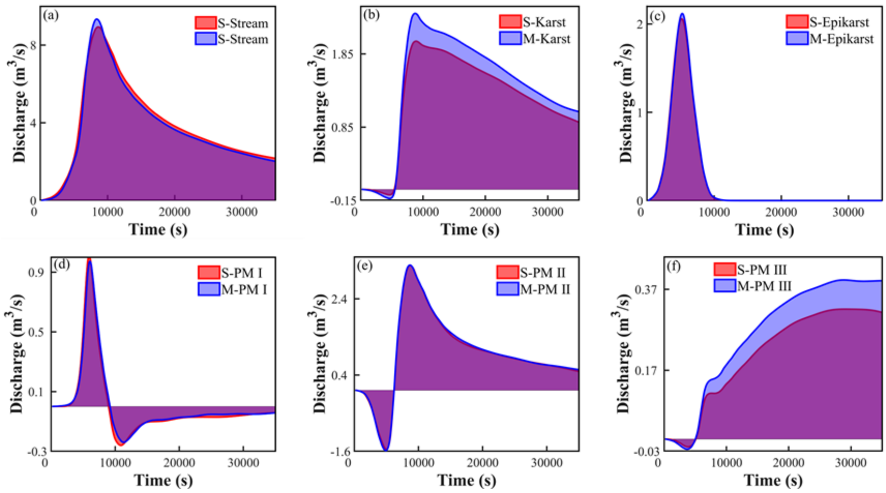

Figure 7. Impacts of single-stage and multi-stage conduit hydrological process changes in various media of the karst aquifer for a precipitation intensity $b = 5$.

https://doi.org/10.5194/egusphere-2025-324
Preprint. Discussion started: 17 February 2025

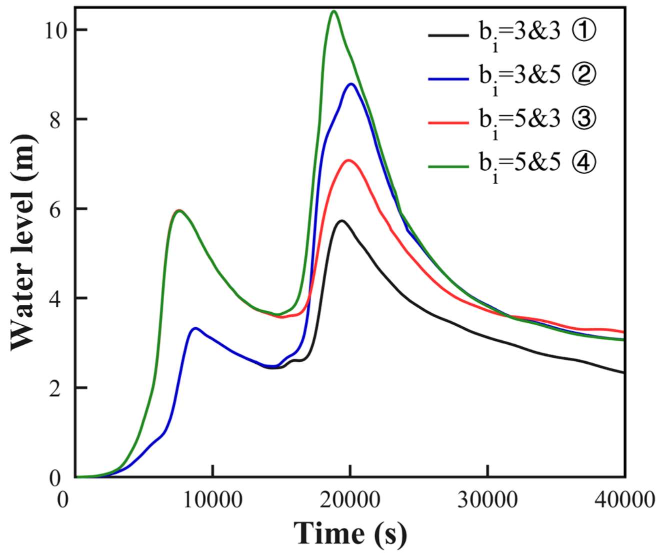

Figure 8. Water levels in stream for two consecutive precipitation events with first and second precipitation intensities ① $b_1 = 3$ and $b_2 = 3$; ② $b_1 = 3$ and $b_2 = 5$; ③ $b_1 = 5$ and $b_2 = 3$; ④ $b_1 = 5$ and $b_2 = 5$, respectively.

https://doi.org/10.5194/egusphere-2025-324
Preprint. Discussion started: 17 February 2025

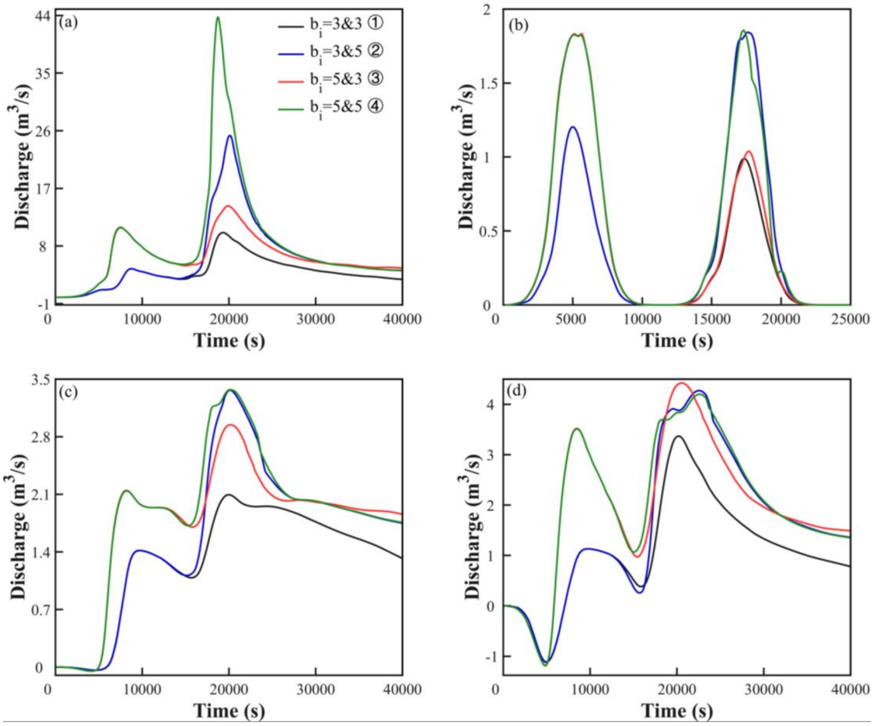

Figure 9. (a) Hydrological process curves of the stream; (b) Discharge process of groundwater through the epikarst to the stream; (c) Discharge process of groundwater through the karst conduit to the stream; (d) Discharge process of porous media (PM II) to the stream, for two consecutive precipitation events with first and second precipitation intensities ① $b_1 = 3$ and $b_2 = 3$; ② $b_1 = 3$ and $b_2 = 5$; ③ $b_1 = 5$ and $b_2 = 3$; ④ $b_1 = 5$ and $b_2 = 5$, respectively.

https://doi.org/10.5194/egusphere-2025-324
Preprint. Discussion started: 17 February 2025

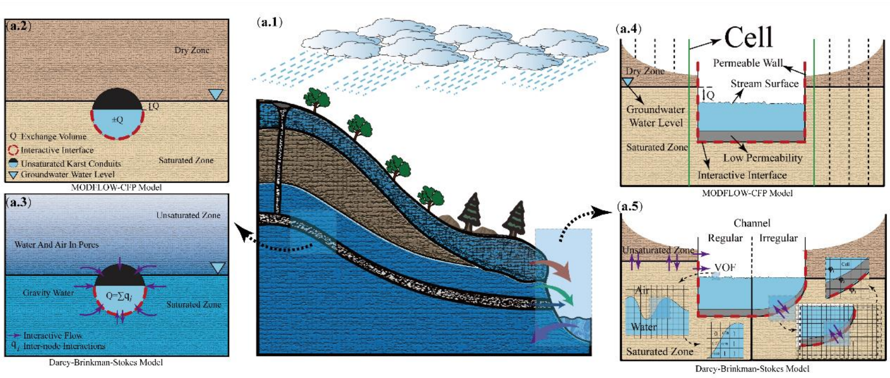

Figure 10. The differences in the interaction patterns of groundwater between conduit and porous media in (a) the MODFLOW-CFP model and (b) the Darcy-Brinkman-Stokes model.

https://doi.org/10.5194/egusphere-2025-324
Preprint. Discussion started: 17 February 2025

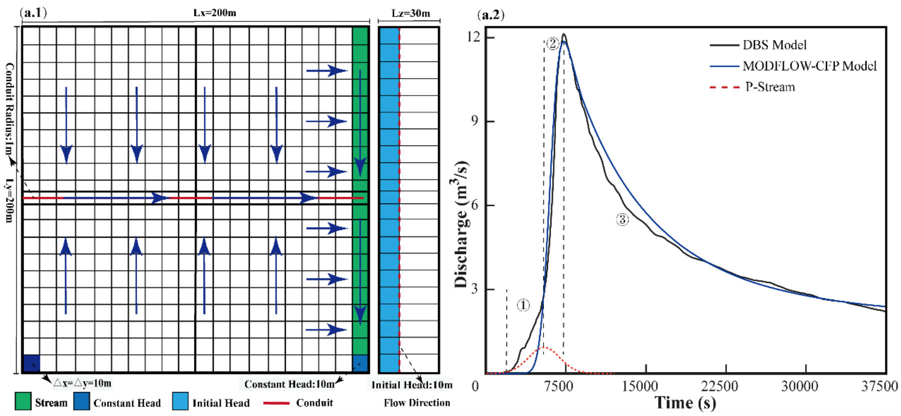

Figure 11. (a.1) Mesh division of the x-y plane and y-z plane of the MODFLOW-CFP two-dimensional model. (b.1) Comparison of the hydrographs of the stream for the MODFLOW-CFP model and the Darcy-Brinkman-Stokes model under the rainfall boundary condition when b = 5.

https://doi.org/10.5194/egusphere-2025-324
Preprint. Discussion started: 17 February 2025

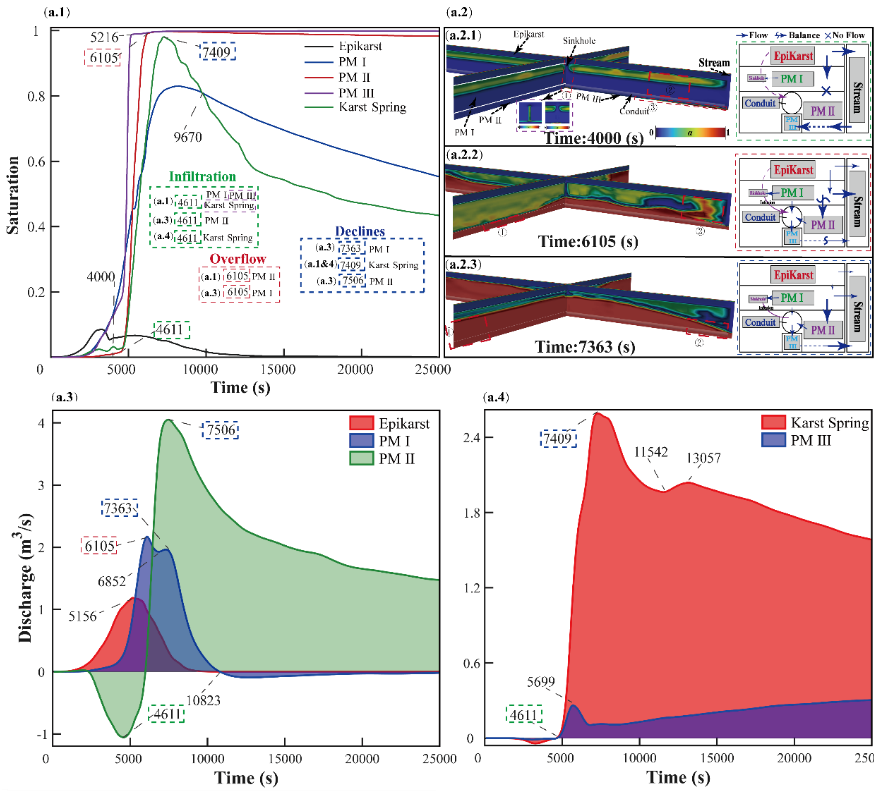

Figure 12. For the Darcy-Brinkman-Stokes model: (a.1) Variations in the saturation levels of epikarst, various porous media, and the karst spring. (a.2) Saturation fields and the interaction among different media at 4000 s, 6105 s, and 7363 s. (a.3) Interaction volumes between epikarst, porous media I, II, and the stream. (a.4) Interaction volumes among the karst spring, porous media III, and the stream.